Available online at www.sciencedirect.com
ScienceDirect
Journal of Hazardous Materials 158 (2008) 35–42
Journal of Hazardous Materials
www.elsevier.com/locate/jhazmat

Phosphate removal from wastewater using red mud

Weiwei Huang [a], Shaobin Wang [b,*], Zhonghua Zhu [a,*], Li Li [a], Xiangdong Yao [a], Victor Rudolph [a], Fouad Haghseresht [a]

[a] *ARC Centre of Excellence for Functional Nanomaterials and Division of Chemical Engineering, The University of Queensland, St Lucia, QLD 4072, Australia*
[b] *Department of Chemical Engineering, Curtin University of Technology, GPO Box U1987, Perth, WA 6845, Australia*

Received 10 September 2007; received in revised form 15 January 2008; accepted 15 January 2008
Available online 1 February 2008

Abstract

Red mud, a waste residue of alumina refinery, has been used to develop effective adsorbents to remove phosphate from aqueous solution. Acid and acid-thermal treatments were employed to treat the raw red mud. The effects of different treatment methods, pH of solution and operating temperature on adsorption have been examined in batch experiments. It was found that all activated red mud samples show higher surface area and total pore volume as well as higher adsorption capacity for phosphate removal. The red mud with HCl treatment shows the highest adsorption capacity among all the red mud samples, giving adsorption capacity of 0.58 mg P/g at pH 5.5 and 40 °C. The adsorption capacity of the red mud adsorbents decreases with increase of pH. At pH 2, the red mud with HCl treatment exhibits adsorption of 0.8 mg P/g while the adsorption can be lowered to 0.05 mg P/g at pH 10. However, the adsorption is improved at higher temperature by increasing 25% from 30 to 40 °C. The kinetic studies of phosphate adsorption onto red mud indicate that the adsorption mainly follows the parallel first-order kinetics due to the presence of two acidic phosphorus species, $H_2PO_4^-$ and HPO_4^{2-}. An analysis of the adsorption data indicates that the Freundlich isotherm provides a better fitting than the Langmuir model.

Keywords: Red mud; Phosphorus removal; Acid treatment; Acid-heat treatment; Kinetics; Isotherm

1. Introduction

Phosphorus is one of the primary nutrients that cause detrimental eutrophication in aquatic environments. A continuing elevated level of phosphate in water system stimulates the growth of photosynthetic algae and toxic cyanobacteria. Domestic wastewaters have typical phosphate concentration ranging from 10 to 15 mg/l [1]. Agricultural, industrial, household uses and many other human activities are the major sources of phosphate in natural water bodies. In order to respond to the demand for lowering the emission of this nutrient into the environment, various technologies for phosphate removal from wastewater have been investigated. The conventional treatment methods that are employed include biological removal, precipitation, adsorption and ion exchange [1,2]. Some novel techniques have also been developed such as electrodialysis and reverse osmosis [3], However, most of these technologies are disadvantaged by poor operational stability or high economic cost. Adsorption technique utilising solid adsorbents, could find a wide application in phosphate removal due to its high efficiency, relatively inexpensive operation and potential for saving and recycling phosphate resources. In recent years, considerable attention has been paid to the development of effective and low-cost adsorbents from industrial solid wastes. If inexpensively alternative adsorbents can be developed, it would be beneficial to the environment and have attractive commercial value.

Red mud (RM) is a waste residue formed after the caustic digestion of bauxite during the production of alumina. It is a highly alkaline waste material with pH 10–12.5. The brick red colour of the RM is mainly contributed by the iron impurities [4]. RM is mainly composed of fine particles containing aluminium oxide, iron oxide, silica, titanium oxides and hydroxides [5]. For every tonne of alumina produced, approximately 1 or 2 tonnes (dry weight) of RM residues are generated. Due to the alkaline nature and the chemical and mineralogical species present in

* Corresponding authors.
E-mail addresses: shaobin.wang@curtin.edu.au (S. Wang), z.zhu@uq.edu.au (Z. Zhu).

0304-3894/$ – see front matter © 2008 Elsevier B.V. All rights reserved.
doi:10.1016/j.jhazmat.2008.01.061

the RM, this solid waste causes a significant impact on the environment and proper disposal of the waste RM presents a huge challenge where alumina industries are located. Many attempts have been made over past years to find some practical applications for RM, such as an additive pigment for mortar and concrete [6] and surface treatment for carbon steel [4]. In recent years, investigations have also been extended to develop RM as an adsorbent to remove arsenate [7,8], toxic heavy metals [9–12], dyes [13–15] and phenol [16–18] from aqueous solution.

For phosphate removal, some investigators have used either acid or heat treated RMs as adsorbents [19–22]. Pradhan et al. reported adsorption of phosphate from aqueous solution using HCl activated RM and achieved 80–90% removal efficiency [19]. Altundogan and Tumen [23] studied the acid treatment and heat treatment to bauxite for removal of phosphate and found that the acid treatment of bauxite reduces the phosphate adsorption capability while heat treatment would increase the capacity. Li et al. [21] recently investigated the effects of acidification and heat treatment of raw RM and fly ash on the sorption of phosphate. They found that the sample prepared by using RM stirred with 0.25 M HCl for 2 h (RM0.25), as well as another sample prepared by heating RM at 700 °C for 2 h (RM700), registered the maximum removal of phosphate (99% removal of phosphate). It is seen that acid or heat treatment could produce an effect on phosphate adsorption depending on the material and treatment conditions. However, no further investigation has been reported on combination of acid and heat treatment of RM on phosphate adsorption. Genc-Fuhrman et al. [7,8] reported an investigation of seawater neutralised RM (Bauxsol) further activated by acid treatment or combined HCl washing and heat treatment for arsenic adsorption. The results showed that acid treatment alone, as well as combination with heat treatment increased the removal efficiency, with the combination providing the best removal.

In this paper, we report an investigation of the adsorption properties of RM and various activated RM in phosphate removal from aqueous solution. We investigated the effects of acid treatment using different acids such as HCl and HNO_3 combined with heat treatment on the properties and adsorptive behaviour of the modified RM with aims at understanding of chemical changes of different pre-treatments of RM and the adsorption kinetics and isotherm of activated RMs in phosphate removal from aqueous solution.

2. Experiment

2.1. Adsorbent materials

The waste RM sample used in the present study was provided by the Worsley Alumina, Australia. The chemical compositions of the RM based on dry weight are Fe_2O_3 (60%), Na_2O (16%), Al_2O_3 (15%), TiO_2 (5%) and SiO_2 (5%). Four derived samples were prepared by different acid treatments and acid-thermal treatments. Typically, the solid RM samples were mixed at room temperature for 24 h with 2 M HCl or 2 M HNO_3 solution, respectively at liquid/solid ratio of 20 ml/g. These two samples are referred to as RM–HCl and RM–HNO_3, respectively. After acid treatment, the residue was washed with distilled water and dried overnight at 100 °C. Acid-thermal treatment was carried out by placing the acid pre-treated RM samples in a muffle furnace for calcination at 700 °C in air for 5 h (referred as RM–HCl-700 and RM–HNO_3-700). The temperature ramp rate of the furnace was set to 10 °C/min. The resultant solid samples were then allowed to cool down overnight in the furnace.

2.2. Characterisation

The surface area and total pore volume were obtained by nitrogen adsorption–desorption at the liquid nitrogen temperature (−196 °C) using a Quadrasorb S1 (Quantachrome Corp.) All samples were degassed at 200 °C for 4 h before analysis. The BET equation was applied to determine the surface area. The total pore volume was determined at $P/P_0 = 0.98$.

X-ray diffraction (XRD) patterns of all samples were measured using a Rigaku miniflex diffractormeter with Co Kα radiations generated at 30 kV, 15 mA. Scattering angles were ranged from 2° to 80°, with a scanning speed at 2° per minute.

Microstructure and surface morphology of the adsorbent samples were characterised by a JEOL 6400 field emission scanning electron microscope (SEM) with an accelerating voltage of 12.0 kV at a magnification 1 × 30,000.

Fourier transfer infrared (FT-IR) spectra were collected on a Nicolet 6700 with a resolution of 4 cm^{-1} by using attenuated total reflectance (ATR) technique. The spectrum was scanned from 400 to 4000 cm^{-1}.

2.3. Adsorption studies

The kinetic tests were carried out in batch experimental mode. One gram of solid sample was placed in a large beaker and mixed with 1 l of 1 mg P/L solution at 70 rpm at varying temperatures. Liquid samples were collected at various time intervals and the concentrations of phosphate were determined by a Jasco V-550 UV/vis spectrophotometer at λ_{max} of 710 nm. A calibration curve was obtained by measuring the absorbance of phosphate concentration ranging from 0.01 to 1 mg P/L as the basis to determine the concentration of the samples.

The kinetics and sorption mechanism were evaluated with three different models: the Lagergren equation, a pseudo first-order mechanism; a pseudo second-order mechanism [24]; and a parallel first-order mechanism. The pseudo first-order equation takes the form

$$\log(q_e - q_t) = \log q_e - \frac{k_1 t}{2.303} \quad (1)$$

or alternatively

$$q_t = q_e(1 - e^{-k_1 t}) \quad (2)$$

where q_t is the amount of phosphate adsorbed at time t (mg/g), q_e is the amount of phosphate adsorbed at equilibrium (mg/g) and k_1 is the equilibrium rate constant for pseudo first-order kinetics (min^{-1}).

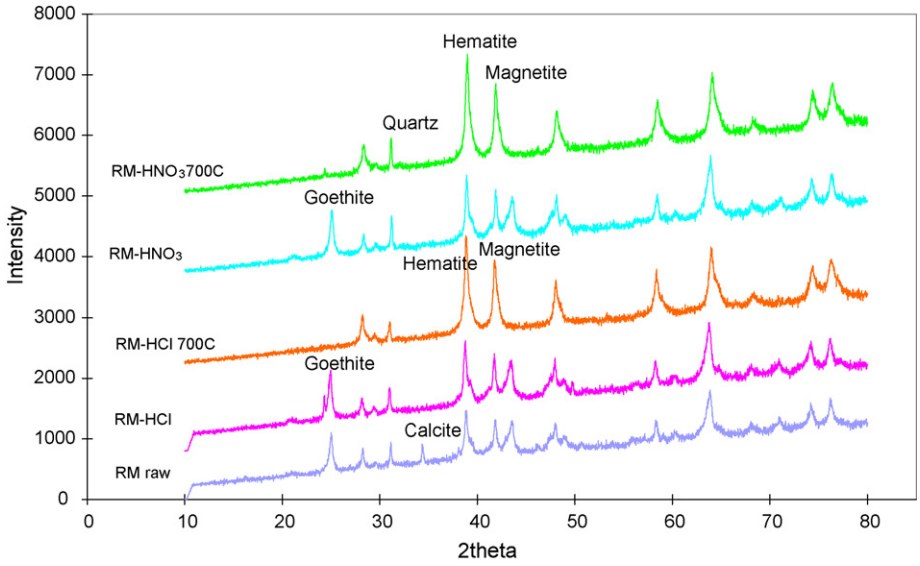

Fig. 1. XRD patterns of RM by different treatments.

The pseudo second-order equation is expressed as

$$\frac{t}{q_t} = \frac{1}{k_2 q_e^2} + \frac{t}{q_e} \tag{3}$$

and can be used in a nonlinear form

$$q_t = \frac{k_2 q_e^2 t}{(1 + k_2 q_e t)} \tag{4}$$

where k_2 is the equilibrium rate constant for the second-order kinetics (g mg^{-1} min^{-1})

The parallel first-order kinetics can be expressed as

$$q_t = q_{e1}(1 - e^{-k_{1a}t}) + q_{e2}(1 - e^{-k_{1b}t}) \tag{5}$$

where q_{e1} and q_{e2} are the amount of phosphate adsorbed at equilibrium (mg/g) in the first and second reactions, respectively, and k_{1a} and k_{1b} (min^{-1}) are the equilibrium rate constants for the first and second reactions, respectively.

The isothermal adsorption tests were performed by shaking 0.02–0.4 g of solid in 50 ml of 1 mg/l KH_2PO_4 (as P) solution at 70 rpm for 6 h at a constant temperature of either 30 or 40 °C. The equilibrium time was determined by the kinetic tests described earlier. The concentration of phosphate was measured using the spectrophotometry described above.

An adsorption isotherm is a mathematical expression of the relationship between the amount of solute adsorbed and the concentration of the solution in the liquid phase at a given constant temperature. In order to determine the mechanism of phosphate adsorption on the RM, two types of isotherms, Langmuir and Freundlich isotherms, were applied to describe the equilibrium adsorption of solutes from liquid solution. The Langmuir isotherm assumes the sorption process at specific homogeneous sites for monolayer adsorption. The Langmuir isotherm can be expressed in the form

$$Q = \frac{kQ_m C_{eq}}{1 + bC_{eq}} \tag{6}$$

where Q is the adsorbed amount of the solute in mg/g, C_{eq} is the equilibrium concentration of the liquid solution in mg/l, Q_m is the monolayer adsorption capacity (mg/g) and k is a constant related to the free energy of adsorption (l/mg).

The Freundlich isotherm is an empirical equation employed to describe heterogeneous system. The Freundlich isotherm can be expressed as

$$Q = KC_{eq}^{1/n} \tag{7}$$

where K is a constant that indicates the extent of the adsorption and n is a constant, which indicates the nonlinearity between solution concentration and the adsorption.

In addition, the effect of pH on adsorption capacity was also investigated. A series of phosphate solution were prepared by adjusting pH over a range of 2–10 using 0.1 M HCl or NaOH solution. The pH of solutions was measured with a pH meter (TPS pH Cube).

3. Result and discussion

3.1. Characteristics of adsorbents

The crystalline phases of RM samples determined by XRD analysis are shown in Fig. 1. In raw RM, the major phases are quartz, hematite, goethite and calcite. The XRD patterns show a remarkable difference between acid treated samples and the acid-thermally treated samples, which suggests that phase trans-

Table 1
Surface area and pore volume of various samples

Samples	S_{BET} (m^2/g)	V_{total} (cm^3/g)
RM	22.71	0.0566
RM–HCl	28.48	0.0779
RM–HCl-700	33.78	0.0928
RM–HNO_3	38.15	0.0658
RM–HNO_3-700	33.33	0.0973

formation has taken place. After acid treatments, the calcite phase present in the raw RM disappears. The acid-thermal treatment creates a new phase of magnetite, which is attributed to the decomposition of goethite. The intensities of hematite also show a significant enhancement, making them the dominant phases in RM–HCl-700 and RM–HNO_3-700 samples.

The BET surface area and total pore volume of various RM samples are given in Table 1. As seen, the raw RM has a surface area of 22.7 m^2/g with pore volume of 0.0566 cm^3/g. Both acid treatments increase the surface area and the pore volume, but RM–HNO_3 shows a larger BET surface area than that of RM–HCl. After thermal treatment, RM–HCl-700 shows a further enhancement in the surface area and pore volume while RM–HNO_3-700 shows a reduction in the surface area.

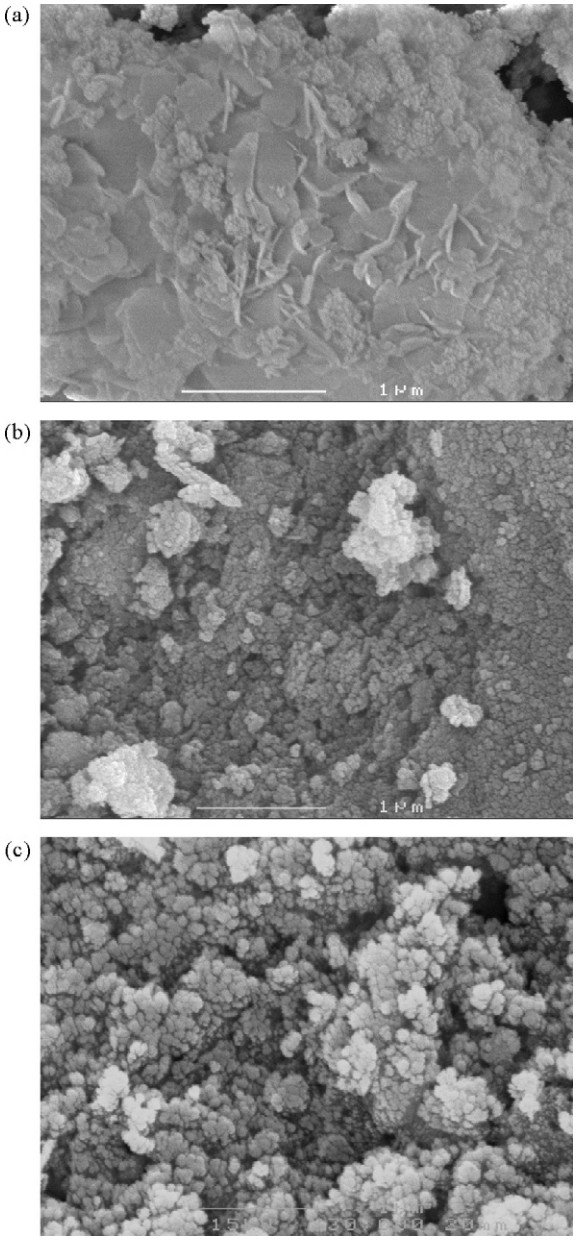

Fig. 2. SEM photographs of RM. (a) Raw RM, (b) RM–HCl and (c) RM–HCl-700.

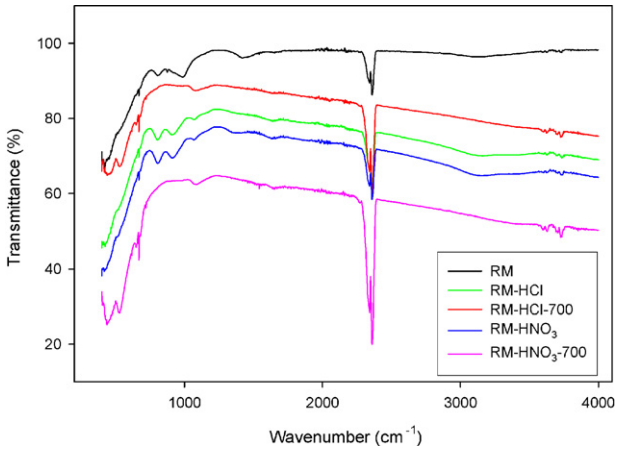

Fig. 3. FT-IR spectra of various RM samples.

SEM pictures provide surface morphology of the RM samples at micro-scale. From Fig. 2, the contrast in surface features between the raw RM which is relatively smooth and flat, and the acid treated specimen, RM–HCl, provides clear visual evidence for the new surface area generated by strong acid treatment. The acid treated sample shows many new cavities and coarsened exterior probably due to removal of some acid-soluble salts [25]. After heat treatment, RM–HCl-700 exhibits a morphology similar to the RM–HCl but with additional porosity.

FT-IR spectra of the differently treated RM samples are presented in Fig. 3. The broad peak at 3130–3450 cm^{-1} corresponding to OH vibrations, appears for RM, RM–HCl and RM–HNO_3. Two intense hydroxyl deformation bands at 906–910 and 802–806 cm^{-1} are seen on RM–HCl and RM–HNO_3 but not observed on RM–HCl-700 and RM–HNO_3-700. This is ascribed to the decomposition of goethite to hematite, confirmed by the appearance of peaks at 439–442 and 528–532 cm^{-1}, which are characteristic vibrations of hematite, and magnetite. Thus, FT-IR results support the evidence of phase change from the XRD profiles.

3.2. Dynamic adsorption of phosphate on RM

Fig. 4 illustrates the results of dynamic adsorption of phosphate on various treated RM samples at natural pH. The adsorption of phosphate onto the RM surface takes place quickly in the first 3 h and attains 85–90% phosphate removal. In the last 3 h, the phosphate uptake becomes much slower until it reaches equilibrium. This is due to the decreased diffusion rate [26]. At approaching equilibrium, adsorbate concentration is much reduced and the saturation of adsorption sites is achieving, the rate of adsorption will be much slow. The time to attain equilibrium for all samples is approximately 6 h. Also as seen from the figure, all treatment methods are able to enhance the adsorption capacity of RM to different levels. Acid treatments by HCl and HNO_3 increase the adsorption and RM–HCl achieves the highest adsorption capacity among all the samples, which suggests that HCl treatment is better than HNO_3 treatment. However, the acid-thermal treatment (RM–HCl-700) shows lower adsorption capacity than RM–HCl. RM–HNO_3 and

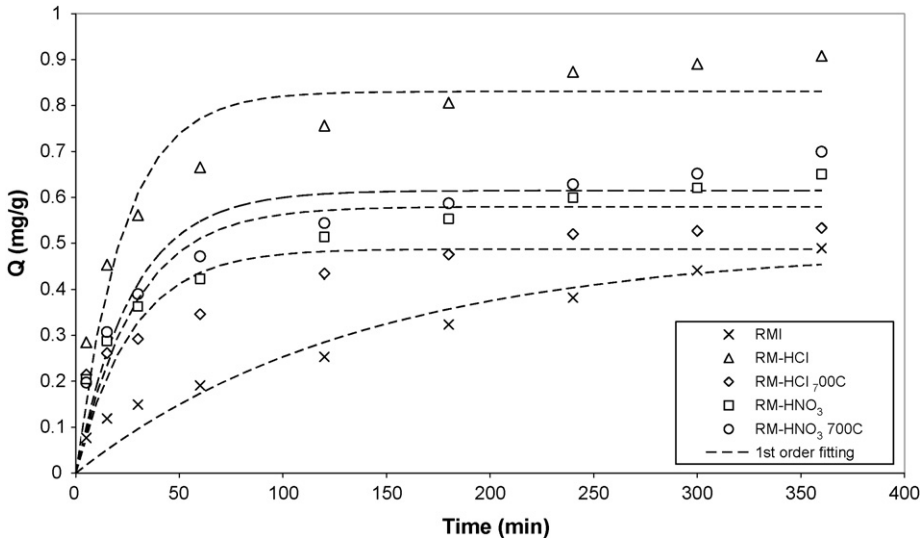

Fig. 4. Pseudo first-order kinetics of phosphate adsorption on different treated RM.

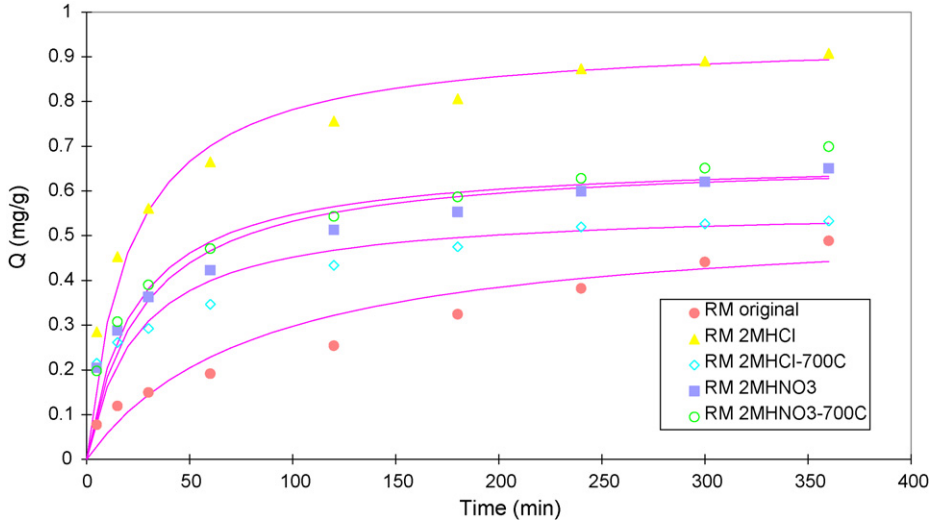

Fig. 5. Pseudo second-order kinetics of phosphate adsorption on different treated RM.

RM–HNO_3-700 exhibits similar adsorption capacity. Generally, acid treatments neutralise the hydroxide ions, which reduces the negative charges on the alkaline surface of RM [13]. The process promotes the adsorption of negatively charged PO_4^{3-} species in solution, thus the increase of adsorption capacity can be anticipated. The high temperature treatment decomposes some organics and hydroxyl groups, which are the effective sites for phosphate adsorption [13]. In addition, heat treatment may also cause the sintering of particles, losing contact area for adsorbate and resulting in low adsorption capacity.

XRD profiles indicate that acid treatment removed calcite from the raw RM, which changes the surface property. N_2 adsorption also demonstrated that BET surface area is increased after acid treatment. During the heat treatment, goethite in the RM was decomposed to form hematite and magnetite, which can be observed from XRD and FT-IR profiles. For RM–HCl-700, the surface area and pore volume are all increased; however, the adsorption is decreased. For RM–HNO_3-700, the surface area is decreased but the pore volume is enhanced while it exhibits similar adsorption to RM–HNO_3. This suggests that the surface area is not important in determining the adsorption capacity. Chemical adsorption would be more important than physical adsorption. Altundogan and Tumen [23] investigated HCl and heat treatments of RM and found that surface area of RM was increased by acid treatment but the treated sample had lowered phosphate adsorption capacity. Parfitt et al. [27] studied the phosphate adsorption on various iron oxides and found that goethite exhibited higher adsorption than hematite. Therefore, it is deduced that RM–HCl exhibits the highest adsorption will be attributed to the stronger chemical interaction of goethite with phosphate and the developed porous structure.

Based on those tests, the experimental results were employed to derive the kinetic parameters using the three different models: the pseudo first-order mechanism, pseudo second-order mechanism, and parallel first-order mechanism. The constants for

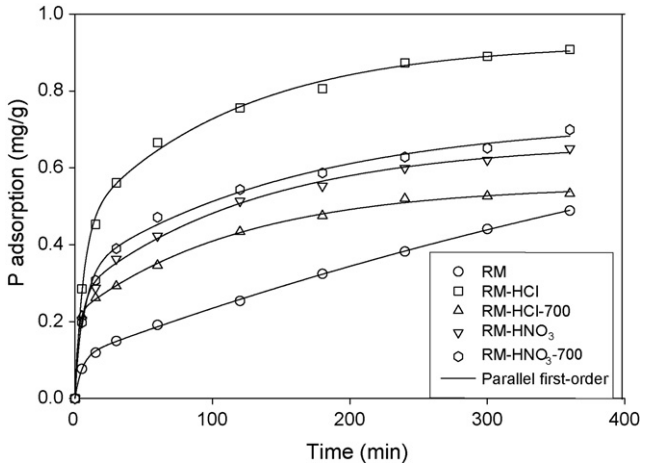

Fig. 6. Parallel first-order kinetics of phosphate adsorption on different RM samples.

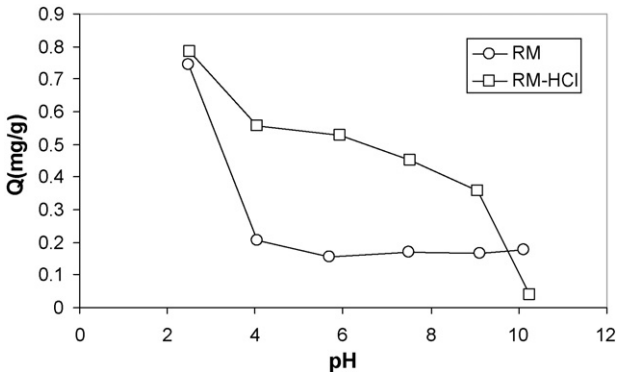

Fig. 7. Effect of pH on phosphate adsorption on raw RM and RM and RM–HCl. $T = 25\,^{\circ}C$.

the three kinetic models were determined by curve fitting with results as shown in Figs. 4–6. The constants are listed in Table 2. It is seen that the first-order kinetics does not show a good agreement with the experimental data whereas the second-order kinetics provides a close fit, with a regression coefficient R^2 of greater than 0.99 in most cases. In adsorption processes, a pseudo second-order mode is generally interpreted to mean that the mechanism of the process is mainly controlled by chemical bonding or chemisorption. This would imply that the cause of phosphate adsorption onto the RM involves valency forces through sharing or exchange of electrons between sorbate and sorbent [28].

However, from the figure and table, it is also seen that the parallel first-order kinetics provides a very good fit of the experimental results. For the two adsorption processes, the adsorption rate in the second process is always lower. This suggests that two active sites are involved in the adsorption. For KH_2PO_4 solution, two acidic phosphorus species, namely $H_2PO_4^-$ and HPO_4^{2-}, may be expected to dominate at natural pH, both of which will be adsorbed on the solid surface. Thus, the mechanism can be described as

$$FeOOH + H_2PO_4^- \rightarrow FeOHPO_4^- + H_2O \quad (8)$$

$$FeOOH + HPO_4^{2-} \rightarrow FeOPO_4^{2-} + H_2O \quad (9)$$

3.3. Effect of pH

RM adsorption capacity has a close relationship with pH value of the phosphate solution as shown in Fig. 7. For both raw RM and RM–HCl over a broad range of pH both materials present a similar trend in that the higher the pH, the lower

Table 2
Parameter for kinetic models of phophate adsorption on various red mud samples

Sample	Parameters				R^2
RM					
Pseudo first-order	$k_1 = 0.0073$	$q_e = 0.489$			0.9816
Pseudo second-order	$k_2 = 0.0222$	$q_e = 0.544$			0.9249
Parallel first-order	$k_{1a} = 0.198$	$q_{e1} = 0.109$	$k_{1b} = 1.39 \times 10^{-3}$	$q_{e2} = 0.965$	0.9996
RM–HCl					
Pseudo first-order	$k_1 = 0.0441$	$q_e = 0.830$			0.9897
Pseudo second-order	$k_2 = 0.0504$	$q_e = 0.946$			0.9974
Parallel first-order	$k_{1a} = 0.164$	$q_{e1} = 0.454$	$k_{1b} = 8.68 \times 10^{-3}$	$q_{e2} = 0.470$	0.9983
RM–HCl-700					
Pseudo first-order	$k_1 = 0.0375$	$q_e = 0.487$			0.9768
Pseudo second-order	$k_2 = 0.0718$	$q_e = 0.564$			0.9946
Parallel first-order	$k_{1a} = 0.500$	$q_{e1} = 0.219$	$k_{1b} = 8.36 \times 10^{-3}$	$q_{e2} = 0.336$	0.9993
RM–HNO_3					
Pseudo first-order	$k_1 = 0.0354$	$q_e = 0.579$			0.9845
Pseudo second-order	$k_2 = 0.0553$	$q_e = 0.675$			0.994
Parallel first-order	$k_{1a} = 0.227$	$q_{e1} = 0.272$	$k_{1b} = 7.60 \times 10^{-3}$	$q_{e2} = 0.393$	0.9978
RM–HNO_3-700					
Pseudo first-order	$k_1 = 0.0369$	$q_e = 0.615$			0.9875
Pseudo second-order	$k_2 = 0.0647$	$q_e = 0.673$			0.9972
Parallel first-order	$k_{1a} = 0.146$	$q_{e1} = 0.329$	$k_{1b} = 6.23 \times 10^{-3}$	$q_{e2} = 0.396$	0.9930

Where $k_1 = \text{min}^{-1}$, $k_2 = \text{g mg}^{-1}\,\text{min}^{-1}$ and $q_e = \text{mg/g}$.

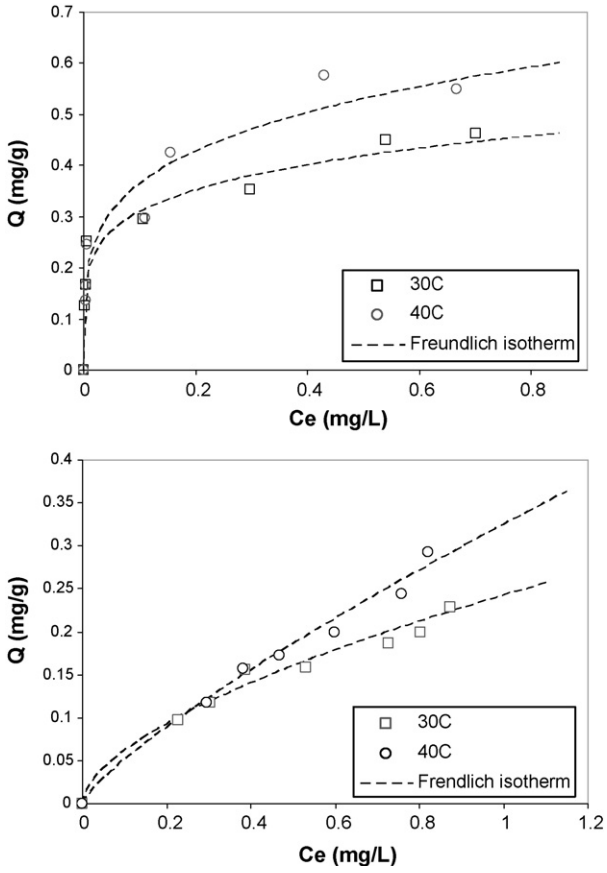

Fig. 8. Effect of temperature on adsorption (a) RM–HCl and (b) RM.

the adsorption capacity. Significant enhancement of adsorption capacities is achieved at a pH of about 2 where the adsorption capacity is about 6 times the amount at pH of 10. A remarkable observation from the pH tests was that, the raw RM at very low pH exhibits similar phosphate removal ability as the acid treated RM. The reason may be attributed to alkaline properties of RM surface, which results in higher adsorption of acid ions. Previous research has demonstrated that increasing the pH results in reduced phosphate adsorption [19]. When the solution has a higher pH, the surface of the RM carries more negative charges which serves to increase the repulsion of the negatively charged phosphate species in solution and consequently results in lower RM adsorption capacity.

3.4. Adsorption isotherm

The adsorption isotherms of RM and RM–HCl at 30 and 40 °C are presented in Fig. 8. The two isotherms, Langmuir and Freundlich isotherms, were applied to describe the equilibrium adsorption of solutes from liquid solution. The isotherm parameters of adsorption using the Langmuir and Freundlich isotherms are also shown in Table 3. It can be seen that the adsorption capacity increases with an increase of temperature, indicative of an endothermic nature of the adsorption. The temperature has more obvious influence on adsorption for RM–HCl while less effect for raw RM. For RM–HCl, the adsorption capacity can achieve up to 0.58 mg P/g at 40 °C, which is increased approximately 25% than that at 30 °C. Raw RM can reach 0.29 mg P/g at 40 °C in comparison with 0.23 mg P/g at 30 °C.

Table 3
Adsorption isotherm parameters for RM–HCl and RM at different temperatures

Sample	Parameters		R^2
RM–HCl 30 °C			
Langmuir model	$k = 545.24$	$Q_m = 0.346$	0.8877
Freundich model	$K = 0.477$	$1/n = 0.1886$	0.9887
RM–HCl 40 °C			
Langmuir model	$k = 146.39$	$Q_m = 0.462$	0.914
Freundich model	$K = 0.623$	$1/n = 0.2336$	0.9098
RM 30 °C			
Langmuir model	$k = 2.73$	$Q_m = 0.271$	0.7967
Freundich model	$K = 0.242$	$1/n = 0.597$	0.9521
RM 40 °C			
Langmuir model	$k = 0.407$	$Q_m = 1.106$	0.9709
Freundich model	$K = 0.325$	$1/n = 0.806$	0.9818

Comparison between experimental data and isotherm models shows that the Freundlich isotherm represents the adsorption process better than the Langmuir isotherm. The higher R^2 value for Freundlich isotherm is also a clear evidence. Since the Freundlich model is more suitable to describe the experimental data, this suggests that some heterogeneity in the surface or pores of adsorbents play a role in the phosphate adsorption.

4. Conclusion

RM has been investigated for removal of phosphate from aqueous solution. Different pre-treatment methods of the RM brought about textural and phase changes, resulting in varying adsorption capacity. Activation of RM with acid treatment or acid-heat treatment increases surface area and thus improves the adsorption capacity. The RM with HCl acid treatment shows the greatest adsorption capacity of 0.58 mg P/g at pH 5.5 and 40 °C while raw RM only presents 0.23 mg P/g at the same conditions. Kinetic and isothermal studies indicate that phosphate adsorption is a heterogeneous adsorption with two major phosphate species. The adsorption kinetics will be best described by the parallel first-order model. The adsorption capacity of each species is similar but adsorption kinetic constants are significantly different. The Freundlich isotherm provides a better fitting to isotherm than the Langmuir isotherm. Both solution pH and temperature will influence the phosphate adsorption on RM. Low solution pH can enhance phosphate adsorption while high solution pH decreases the adsorption. Due to the endothermic nature of phosphate adsorption on RM, high temperature will increase the adsorption capacity. For RM and RM–HCl, the adsorption can both increase by 25% from 30 to 40 °C.

References

[1] L.L. Blackall, G. Crocetti, A.M. Saunders, P.L. Bond, A review and update of the microbiology of enhanced biological phosphorus removal in wastewater treatment plants, Antonie Van Leeuwenhoek Int. J. Gen. Mol. Microbiol. 81 (2002) 681–691.

[2] G. Akay, B. Keskinler, A. Cakici, U. Danis, Phosphate removal from water by red mud using crossflow microfiltration, Water Res. 32 (1998) 717–726.
[3] E. Oguz, Removal of phosphate from aqueous solution with blast furnace slag, J. Hazard. Mater. 114 (2004) 131–137.
[4] A. Collazo, D. Fernandez, M. Izquierdo, X.R. Novoa, C. Perez, Evaluation of red mud as surface treatment for carbon steel prior painting, Prog. Org. Coat. 52 (2005) 351–358.
[5] S. Kumar, R. Kumar, A. Bandopadhyay, Innovative methodologies for the utilisation of wastes from metallurgical and allied industries, Resour. Conserv. Recycl. 48 (2006) 301–314.
[6] J. Pera, R. Boumaza, J. Ambroise, Development of a pozzolanic pigment from red mud, Cement Concrete Res. 27 (1997) 1513–1522.
[7] H. Genc-Fuhrman, J.C. Tjell, D. McConchie, Adsorption of arsenic from water using activated neutralized red mud, Environ. Sci. Technol. 38 (2004) 2428–2434.
[8] H. Genc-Fuhrman, J.C. Tjell, D. McConchie, Increasing the arsenate adsorption capacity of neutralized red mud (Bauxsol), J. Colloid Interface Sci. 271 (2004) 313–320.
[9] M. Vaclavikova, P. Misaelides, G. Gallios, S. Jakabsky, S. Hredzak, Removal of cadmium, zinc, copper and lead by red mud, an iron oxides containing hydro metallurgical waste, in: Oxide Based Materials: New Sources, Novel Phases, New Applications, vol. 155, 2005, pp. 517–525.
[10] E. Lopez, B. Soto, M. Arias, A. Nunez, D. Rubinos, M.T. Barral, Adsorbent properties of red mud and its use for wastewater treatment, Water Res. 32 (1998) 1314–1322.
[11] A.F. Bertocchi, M. Ghiani, R. Peretti, A. Zucca, Red mud and fly ash for remediation of mine sites contaminated with As, Cd, Cu, Pb and Zn, J. Hazard. Mater. 134 (2006) 112–119.
[12] E. Lombi, F.J. Zhao, G.Y. Zhang, B. Sun, W. Fitz, H. Zhang, S.P. McGrath, In situ fixation of metals in soils using bauxite residue: chemical assessment, Environ. Pollut. 118 (2002) 435–443.
[13] S.B. Wang, Y. Boyjoo, A. Choueib, Z.H. Zhu, Removal of dyes from aqueous solution using fly ash and red mud, Water Res. 39 (2005) 129–138.
[14] C. Namasivayam, D.J.S.E. Arasi, Removal of congo red from wastewater by adsorption onto waste red mud, Chemosphere 34 (1997) 401–417.
[15] V.K. Gupta, Suhas, I. Ali, V.K. Saini, Removal of rhodamine B, fast green, and methylene blue from wastewater using red mud, an aluminum industry waste, Ind. Eng. Chem. Res. 43 (2004) 1740–1747.
[16] A. Tor, Y. Cengeloglu, M.E. Aydin, M. Ersoz, Removal of phenol from aqueous phase by using neutralized red mud, J. Colloid Interface Sci. 300 (2006) 498–503.
[17] V.K. Gupta, I. Ali, V.K. Saini, Removal of chlorophenols from wastewater using red mud: an aluminum industry waste, Environ. Sci. Technol. 38 (2004) 4012–4018.
[18] C. Namasivayam, K. Thamaraiselvi, Adsorption of 2-chlorophenol by "waste" red mud, Fresenius Environ. Bull. 7 (1998) 314–319.
[19] J. Pradhan, J. Das, S. Das, R.S. Thakur, Adsorption of phosphate from aqueous solution using activated red mud, J. Colloid Interface Sci. 204 (1998) 169–172.
[20] H.S. Altundogan, F. Tumen, Removal of phosphates from aqueous solutions by using bauxite. I. Effect of pH on the adsorption of various phosphates, J. Chem. Technol. Biotechnol. 77 (2002) 77–85.
[21] Y.Z. Li, C.J. Liu, Z.K. Luan, X.J. Peng, C.L. Zhu, Z.Y. Chen, Z.G. Zhang, J.H. Fan, Z.P. Jia, Phosphate removal from aqueous solutions using raw and activated red mud and fly ash, J. Hazard. Mater. 137 (2006) 374–383.
[22] D.J. Akhurst, G.B. Jones, M. Clark, D. McConchie, Phosphate removal from aqueous solutions using neutralised bauxite refinery residues (Bauxsol (TM)), Environ. Chem. 3 (2006) 65–74.
[23] H.S. Altundogan, F. Tumen, Removal of phosphates from aqueous solutions by using bauxite II: the activation study, J. Chem. Technol. Biotechnol. 78 (2003) 824–833.
[24] Y.S. Ho, C.C. Chiang, Sorption studies of acid dye by mixed sorbents, Adsorp. -J. Int. Adsorp. Soc. 7 (2001) 139–147.
[25] L. Santona, P. Castaldi, P. Melis, Evaluation of the interaction mechanisms between red muds and heavy metals, J. Hazard. Mater. 136 (2006) 324–329.
[26] S. Karaca, A. Gurses, M. Ejder, M. Acikyildiz, Adsorptive removal of phosphate from aqueous solutions using raw and calcinated dolomite, J. Hazard. Mater. 128 (2006) 273–279.
[27] L. Parfitt, J. Atkinson, C. Smart, The mechanism of phosphate fixation by iron oxides, Soil Sci. Soc. Am. Proc. 39 (1977) 837–841.
[28] P.B. Bhakat, A.K. Gupta, S. Ayoob, S. Kundu, Investigations on arsenic(V) removal by modified calcined bauxite, Colloids Surf. A: Physicochem. Eng. Aspects 281 (2006) 237–245.